Available online at www.sciencedirect.com

SCIENCE DIRECT®

JOURNAL OF COMPUTATIONAL AND APPLIED MATHEMATICS

Journal of Computational and Applied Mathematics 175 (2005) 31–40

www.elsevier.com/locate/cam

A duality method for the compressible Reynolds equation. Application to simulation of read/write processes in magnetic storage devices

Iñigo Arregui*, J. Jesús Cendán, Carlos Vázquez

Departamento de Matemàticas, Universidad de A Coruña, Campus de Elviña, 15071-A Coruña, Spain

Received 9 October 2003; received in revised form 10 March 2004

Abstract

In this work the authors present a new numerical algorithm to approximate the solution of compressible Reynolds equation with additional first-order slip flow terms. This equation appears when modelling read/write processes in magnetic storage devices such as hard disks. The proposed numerical method is based on characteristics approximation for convection (dominating) terms and a duality method applied to a maximal monotone operator which represents the nonlinear diffusive term. Several test examples illustrate the good performance of the method.

Keywords: Compressible Reynolds lubrication equation; Characteristics method; Maximal monotone operators; Duality algorithms

1. Introduction

In magnetic storage devices, heads are designed so that a thin air film (air bearing) is generated between the head and the magnetic storage device in the read/write process. In this way, the head–device contact only takes place at the initial and final moments. Thus, once a velocity value is reached, the

* Corresponding author. Tel.: +34-981-167000; fax: +34-981-167160.
E-mail addresses: arregui@udc.es (I. Arregui), suceve@udc.es (J. Jesús Cendán), carlosv@udc.es (C. Vázquez).

doi:10.1016/j.cam.2004.06.009

air film is built up so that the hydrodynamic load balances the external load. As the head–device gap is so thin (0.1 μm for hard-disk devices), hydrodynamic and elastohydrodynamic lubrication theories govern this kind of processes. In the case of hard disk devices, the air pressure is governed by a nonlinear compressible Reynolds equation and the elastic effects are neglected. As in magnetic recording the air gap is very small, a compressible Reynolds equation which takes into account the molecular slip boundary conditions at surfaces has to be considered. In tapes and floppy disks (flexible storage media) the proposed elastohydrodynamic 1D model consists of a coupled system based on the compressible Reynolds equation for air pressure and a rod model for the tape deflection [6].

More precisely, in the case of flexible media, the coupled problem providing the air pressure $\widetilde{p}$, in the thin film and the tape geometry $\widetilde{u}$, is posed in terms of equations [9]:

$$6V\mu \frac{\mathrm{d}}{\mathrm{d}y}(\widetilde{p}\widetilde{h}) - 6\lambda p_{\mathrm{a}} \frac{\mathrm{d}}{\mathrm{d}y}\left(\widetilde{h}^2 \frac{\mathrm{d}\widetilde{p}}{\mathrm{d}y}\right) - \frac{\mathrm{d}}{\mathrm{d}y}\left(\widetilde{h}^3 \widetilde{p} \frac{\mathrm{d}\widetilde{p}}{\mathrm{d}y}\right) = 0 \quad \text{in } (\widetilde{L}_1, \widetilde{L}_2), \tag{1.1}$$

$$-(T-\rho V^2)\frac{\mathrm{d}^2\widetilde{u}}{\mathrm{d}y^2} + \mathrm{EI}\frac{\mathrm{d}^4\widetilde{u}}{\mathrm{d}y^4} = (\widetilde{p} - p_{\mathrm{a}})\kappa_{[\widetilde{L}_1, \widetilde{L}_2]} \quad \text{in } (0, \widetilde{L}), \tag{1.2}$$

$$\widetilde{h} = \widetilde{u} - \widetilde{\delta} \geqslant 0 \quad \text{in } (\widetilde{L}_1, \widetilde{L}_2), \tag{1.3}$$

$$\widetilde{p}(\widetilde{L}_1) = \widetilde{p}(\widetilde{L}_2) = p_{\mathrm{a}}, \tag{1.4}$$

$$\widetilde{u}(0) = \widetilde{u}(\widetilde{L}) = \frac{\mathrm{d}\widetilde{u}}{\mathrm{d}y}(0) = \frac{\mathrm{d}\widetilde{u}}{\mathrm{d}y}(\widetilde{L}) = 0, \tag{1.5}$$

where $\widetilde{h}$ is the head–media gap, V denotes the tape velocity, λ the particle mean-free length, p_{a} the ambient pressure and μ the air viscosity. Moreover, T, ρ, E and I represent the tension, the density, Young modulus and the inertia moment of the tape, respectively. The ends of the tape are placed at $y=0$ and $\widetilde{L}$ while the edges of the head are located at $y = \widetilde{L}_1$ and $\widetilde{L}_2$, respectively. The coupled feature results from the definition of the gap, $\widetilde{h} = \widetilde{u} - \widetilde{\delta}$, $\widetilde{\delta}$ being the head geometry, and from the pressure acting as a normal force on the flexible tape (1.2). The notation κ_C holds for the characteristic function of the set C. Typical values of the involved physical parameters are [13]:

$$V = 2.54\ \mathrm{m/s}, \quad \widetilde{L}_1 = 0.0347\ \mathrm{m}, \quad \widetilde{L}_2 = 0.0497\ \mathrm{m}, \quad \widetilde{L} = 0.0843\ \mathrm{m},$$
$$\mu = 1.81 \times 10^{-5}\ \mathrm{kg/s\ m}, \quad \lambda = 6.35 \times 10^{-8}\ \mathrm{m}, \quad p_{\mathrm{a}} = 84100\ \mathrm{N/m^2},$$
$$T = 277\ \mathrm{N/m}, \quad \rho = 0.0207\ \mathrm{kg/m^2}, \quad \mathrm{EI} = 1.52 \times 10^{-5}\ \mathrm{N\ m}.$$

Moreover, usual values for the head radius and the maximum penetration are 0.0204 and 0.00635 m, respectively.

The mathematical analysis for the compressible Reynolds equation has been the subject of several papers in the steady state [8] and unsteady cases [12,14]. Moreover, in [11] two-scale techniques provide asymptotic models to take into account the presence of periodic asperities on the hard-disk surface. In the case of flexible storage devices, the mathematical analysis for the model (1.1)–(1.5) is presented in [10]. This analysis starts from the following change of unknowns and variables:

$$x = 100\,y, \quad p = \widetilde{p}/p_{\mathrm{a}}, \quad u = 10^6\,\widetilde{u}, \quad h = 10^6\,\widetilde{h}, \quad \delta = 10^6\,\widetilde{\delta},$$

which leads to the system

$$\frac{\mathrm{d}}{\mathrm{d}x}(ph) - \varepsilon \frac{\mathrm{d}}{\mathrm{d}x}\left(\alpha h^2 \frac{\mathrm{d}p}{\mathrm{d}x} + \beta h^3 p \frac{\mathrm{d}p}{\mathrm{d}x}\right) = 0 \quad \text{in } (L_1, L_2), \tag{1.6}$$

$$-\frac{\mathrm{d}^2 u}{\mathrm{d}x^2} + \eta \frac{\mathrm{d}^4 u}{\mathrm{d}x^4} = K\,(p-1)\kappa_{[L_1, L_2]} \quad \text{in } (0, L), \tag{1.7}$$

$$h = u - \delta \geqslant 0 \quad \text{in } (L_1, L_2), \tag{1.8}$$

$$p(L_1) = p(L_2) = 1, \tag{1.9}$$

$$u(0) = u(L) = \frac{\mathrm{d}u}{\mathrm{d}x}(0) = \frac{\mathrm{d}u}{\mathrm{d}x}(L) = 0, \tag{1.10}$$

where

$$\alpha = 10^{-4}\,\frac{\lambda p_{\mathrm{a}}}{\varepsilon \mu V}, \quad \beta = 10^{-10}\,\frac{p_{\mathrm{a}}}{6\varepsilon\mu V}, \quad \eta = 10^4\,\frac{\mathrm{EI}}{T - \rho V^2}, \quad K = 10^2\,\frac{p_{\mathrm{a}}}{T - \rho V^2}.$$

Concerning the numerical methods, finite differences schemes are used in [13] for the numerical simulation of a model very close to (1.1)–(1.5), with not enough justified technical strategies. In the more recent paper [11], a LPDEM discretization scheme, combined with a Newton–Raphson technique, is applied to the compressible Reynolds equation and the corresponding two-scale limit models.

In this paper, we mainly focus on a new numerical solution of the hydrodynamic part of the coupled problem. More precisely, we propose a linearization procedure for the compressible Reynolds equation based on duality methods for nonlinear maximal monotone operators.

Thus, the outline of the present work is as follows. In Section 2 the hydrodynamic mathematical model is posed. In Section 3, the numerical algorithm is detailed. Finally, some numerical results are shown in Section 4; in particular, a first example provided of an analytical solution, and a second test issued from the literature illustrate the good performance of the numerical method.

2. The hydrodynamic mathematical model

In this work, only the nonlinear boundary value problem associated with Eq. (1.6) has to be solved. So, for a given gap function h (we can assume a regularity $h \in C^1(L_1, L_2)$) and given parameters ε, α, β, L_1 and L_2, we have to compute the scaled pressure p, as the solution of

$$\frac{\mathrm{d}}{\mathrm{d}x}(ph) - \varepsilon \frac{\mathrm{d}}{\mathrm{d}x}\left(\alpha h^2 \frac{\mathrm{d}p}{\mathrm{d}x} + \beta h^3 p \frac{\mathrm{d}p}{\mathrm{d}x}\right) = 0, \quad \text{in } (L_1, L_2), \tag{2.11}$$

$$p(L_1) = p(L_2) = 1. \tag{2.12}$$

Notice that, for the usual physical values involved, diffusion coefficients $\varepsilon\alpha$ and $\varepsilon\beta$ are of order 10^{-3} and 10^{-2}, respectively. So, we have a convection dominated problem with, in addition, a nonlinear diffusive term. In order to overcome these difficulties, we propose in the next section a characteristics method for the convection dominated aspect and a duality method for the nonlinearity.

In order to develop a finite element spatial discretization, we first pose an adequate variational formulation. For this, we introduce the following functional spaces and sets:

$$V = H^1(L_1, L_2), \quad V_0 = H_0^1(L_1, L_2), \quad V_1 = \{\varphi \in V \,/\, \varphi(L_1) = \varphi(L_2) = 1\}.$$

So, the variational formulation of the hydrodynamic problem can be written as:

Find $p \in V_1$ such that

$$\int_{L_1}^{L_2} \frac{\mathrm{d}(ph)}{\mathrm{d}x}\,\varphi\,\mathrm{d}x + \varepsilon\alpha \int_{L_1}^{L_2} h^2 \frac{\mathrm{d}p}{\mathrm{d}x}\frac{\mathrm{d}\varphi}{\mathrm{d}x}\,\mathrm{d}x + \varepsilon\beta \int_{L_1}^{L_2} h^3\, p \frac{\mathrm{d}p}{\mathrm{d}x}\frac{\mathrm{d}\varphi}{\mathrm{d}x}\,\mathrm{d}x = 0, \quad \forall\varphi \in V_0. \tag{2.13}$$

In the next section, we describe the proposed numerical methods to approximate the solution of (2.13).

3. Numerical algorithm

3.1. The characteristics method

Although characteristics method has been introduced for parabolic and hyperbolic problems in [2], the convergence of the steady version of the method has been stated in [1] for a particular lubrication problem. For a steady problem, this method introduces an artificial dependence on a time variable t, so that

$$\bar{p}(x,t) = p(x), \quad \bar{h}(x,t) = h(x).$$

If we assume an artificial velocity field $v(x) = 1$, we have the following identities for the total derivative:

$$\frac{\mathrm{D}(\bar{p}\bar{h})}{\mathrm{D}t}(x,t) = \frac{\partial(\bar{p}\bar{h})}{\partial t}(x,t) + v(x)\frac{\partial(\bar{p}\bar{h})}{\partial x}(x,t) = \frac{\partial(ph)}{\partial x}(x,t),$$

where $\mathrm{D}/\mathrm{D}t$ represents the material derivative along the characteristic line

$$\tau \to \chi(x,t;\tau),$$

which is the unique solution of the final value problem

$$\frac{\mathrm{d}\chi}{\mathrm{d}\tau}(x,t;\tau) = v(\chi(x,t;\tau)) = 1,$$
$$\chi(x,t;t) = x.$$

In order to discretize the total derivative, for an artificial time step k we denote $\chi^k(x) = \chi(x,t;t-k)$ the position of a material particle in the instant $t-k$. Notice that, taking into account the value of artificial velocity, $\chi(\tau) = x + \tau - t$ is straightforwardly obtained.

So, we approximate the material derivative by a first-order quotient

$$\begin{aligned}\frac{\mathrm{D}(\bar{p}\bar{h})}{\mathrm{D}t}(x,t) &\approx \frac{(\bar{p}\bar{h})(x,t) - (\bar{p}\bar{h})(\chi^k(x), t-k)}{k} \\ &= \frac{(ph)(x) - (ph)(\chi^k(x))}{k} = \frac{(ph)(x) - (ph)(x-k)}{k}\end{aligned}$$

and, after substitution in (2.13), we propose to obtain the steady pressure p, as the limit of the sequence $\{p^m\}$, which is defined by the following algorithm:

For p^m given, find $p^{m+1} \in V_1$ such that:

$$\int_{L_1}^{L_2} p^{m+1} h\varphi \, \mathrm{d}x + k\varepsilon \int_{L_1}^{L_2} \left(\alpha h^2 \frac{\mathrm{d}p^{m+1}}{\mathrm{d}x} + \beta h^3 p^{m+1} \frac{\mathrm{d}p^{m+1}}{\mathrm{d}x} \right) \frac{\mathrm{d}\varphi}{\mathrm{d}x} \, \mathrm{d}x$$
$$= \int_{L_1}^{L_2} ((p^m h) \circ \chi^k)\varphi \, \mathrm{d}x, \quad \forall \varphi \in V_0. \tag{3.14}$$

Notice that, for each index m, (3.14) is a nonlinear diffusion problem depending on the time step k.

3.2. The duality algorithm

Next, in order to overcome the difficulty due to the nonlinear diffusive term in (3.14), we make use of Bermúdez–Moreno algorithm [3,5]. This duality algorithm is based on the introduction of Lagrange multipliers and the approximation of a nonlinear maximal monotone operator by means of its Yosida regularization. In our case, we consider the maximal monotone operator f defined by

$$f(p) = \begin{cases} 0 & \text{if } p < 0, \\ p^2 & \text{if } p \geqslant 0, \end{cases}$$

so that the hydrodynamic equation (3.14) can be written in the form:

$$\int_{L_1}^{L_2} p^{m+1} h\varphi \, \mathrm{d}x + k\varepsilon \int_{L_1}^{L_2} \left(\alpha h^2 \frac{\mathrm{d}p^{m+1}}{\mathrm{d}x} + \frac{\beta h^3}{2} \frac{\mathrm{d}f(p^{m+1})}{\mathrm{d}x} \right) \frac{\mathrm{d}\varphi}{\mathrm{d}x} \, \mathrm{d}x$$
$$= \int_{L_1}^{L_2} ((p^m h) \circ \chi^k)\varphi \, \mathrm{d}x, \quad \forall \varphi \in V_0. \tag{3.15}$$

Next, we introduce a parameter $\omega > 0$ and the new unknown θ

$$\theta = f(p) - \omega p = (f - \omega I)(p),$$

so that

$$f(p) = \theta + \omega p \quad \text{and} \quad \frac{\mathrm{d}f(p)}{\mathrm{d}x} = \frac{\mathrm{d}\theta}{\mathrm{d}x} + \omega \frac{\mathrm{d}p}{\mathrm{d}x}.$$

Now, we apply Bermúdez–Moreno lemma [5]

$$\theta = f(p) - \omega p \quad \Leftrightarrow \quad \theta = f_\lambda^\omega(p + \lambda\theta),$$

where f_λ^ω is the Yosida approximation of the operator $A_\omega = f - \omega I$, which is given by

$$f_\lambda^\omega(s) = \frac{I - J_\lambda(s)}{\lambda},$$

$J_\lambda = (I + \lambda A_\omega)^{-1}$ being the resolvent operator [7]. For convergence purposes, we will take $2\lambda\omega = 1$.

So, in order to build up the method, we first get the resolvent operator. Thus, for $s \in \mathbb{R}$, let $t = J_\lambda(s)$, that is

$$t = J_\lambda(s) = (I + \lambda(f - \omega I))^{-1}(s)$$

or equivalently

$$s = t + \lambda(f - \omega I)t = \begin{cases} t - \lambda\omega t & \text{if } t < 0, \\ t + \lambda t^2 - \lambda\omega t & \text{if } t \geqslant 0. \end{cases}$$

Therefore, from easy computations, we get for $2\lambda\omega = 1$

$$J_{1/2\omega}(s) = \begin{cases} 2s & \text{if } s < 0, \\ -\dfrac{\omega}{2} + \dfrac{1}{2}\sqrt{\omega^2 + 8\omega s} & \text{if } s \geqslant 0. \end{cases}$$

Next, we deduce the following expression of the Yosida approximation:

$$f^{\omega}_{1/2\omega}\left(p + \frac{\theta}{2\omega}\right) = \begin{cases} -\theta - 2\omega p & \text{if } p + \dfrac{\theta}{2\omega} \leqslant 0, \\ \theta + 2\omega p + \omega^2 - \omega\sqrt{4\theta + 8\omega p + \omega^2} & \text{if } p + \dfrac{\theta}{2\omega} \geqslant 0. \end{cases}$$

At this stage, we have to remark that the experimentally observed convergence of Bermúdez–Moreno algorithm strongly depends on the choice of the parameter ω which, in turn, depends on the exact solution. In [15], some strategies for the optimal choice of the parameters are proposed.

Finally, the variational formulation of the hydrodynamic problem is:

Find $(p^{m+1}, \theta^{m+1}) \in V_1 \times V_1$ such that

$$\int_{L_1}^{L_2} p^{m+1}\, h\, \varphi\, \mathrm{d}x + k\varepsilon \int_{L_1}^{L_2} \left(\alpha h^2 \frac{\mathrm{d}p^{m+1}}{\mathrm{d}x} + \frac{\beta\omega}{2} h^3 \frac{\mathrm{d}p^{m+1}}{\mathrm{d}x}\right) \frac{\mathrm{d}\varphi}{\mathrm{d}x}\, \mathrm{d}x$$
$$= \int_{L_1}^{L_2} ((p^m h) \circ \chi^k)\varphi\, \mathrm{d}x - \frac{k\varepsilon\beta}{2} \int_{L_1}^{L_2} h^3 \frac{\mathrm{d}\theta^{m+1}}{\mathrm{d}x} \frac{\mathrm{d}\varphi}{\mathrm{d}x}\, \mathrm{d}x, \quad \forall \varphi \in V_0,$$
$$\theta^{m+1} = f^{\omega}_{1/2\omega}\left(p^{m+1} + \frac{1}{2\omega}\theta^{m+1}\right),$$

where the nonlinear aspect still remains.

In order to approximate the solution of the previous problem, we propose the following fixed point algorithm:

- For $\theta^{m+1,\ell}$ known, compute $p^{m+1,\ell+1}$ as the solution of the linear problem

$$\int_{L_1}^{L_2} p^{m+1,\ell+1}\, h\, \varphi\, \mathrm{d}x + k\varepsilon \int_{L_1}^{L_2} \left(\alpha h^2 \frac{\mathrm{d}p^{m+1,\ell+1}}{\mathrm{d}x} + \frac{\beta\omega}{2} h^3 \frac{\mathrm{d}p^{m+1,\ell+1}}{\mathrm{d}x}\right) \frac{\mathrm{d}\varphi}{\mathrm{d}x}\, \mathrm{d}x$$
$$= \int_{L_1}^{L_2} ((p^m h) \circ \chi^k)\varphi\, \mathrm{d}x - \frac{k\varepsilon\beta}{2} \int_{L_1}^{L_2} h^3 \frac{\mathrm{d}\theta^{m+1,\ell}}{\mathrm{d}x} \frac{\mathrm{d}\varphi}{\mathrm{d}x}\, \mathrm{d}x, \quad \forall \varphi \in V_0. \tag{3.16}$$

- Update the multiplier $\theta^{m+1,\ell+1}$ by means of

$$\theta^{m+1,\ell+1} = f^{\omega}_{1/2\omega}\left(p^{m+1,\ell+1} + \frac{1}{2\omega}\theta^{m+1,\ell}\right).$$

For the spatial discretization of the linear problem (3.16), piecewise linear Lagrange finite elements have been employed on a uniform mesh. Moreover, adequate Gauss formulae for numerical quadrature in the different terms have been used.

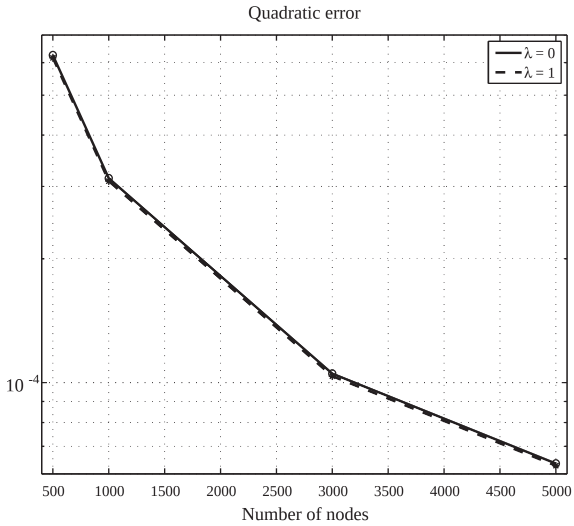

Fig. 1. Quadratic error for Test 1 with different uniform meshes.

4. Numerical results

In order to validate the previous algorithm, we have performed two numerical tests that illustrate its good behaviour. In the first one, we solve a problem provided with an analytical solution; the second one, more realistic, is proposed in Jai [11].

Test 1. For the given parameters λ and Λ, let us consider the problem

$$\Lambda \frac{\mathrm{d}}{\mathrm{d}x}(h\,p) - \frac{\mathrm{d}}{\mathrm{d}x}\left(\lambda h^2 \frac{\mathrm{d}p}{\mathrm{d}x} + h^3 p \frac{\mathrm{d}p}{\mathrm{d}x}\right) = f, \quad x \in (0,1),$$
$$p(0) = p(1) = 1$$

which corresponds to the choice

$$\alpha = \frac{\lambda}{\varepsilon\Lambda}, \quad \beta = \frac{1}{\varepsilon\Lambda}, \quad L_1 = 0, \quad L_2 = 1$$

in Eq. (2.11). The gap is given by $h(x) = 2 - x$ and f is a function so that the solution of the boundary value problem (2.11)–(2.12) is the polynomial $p(x) = 1 + x - x^2$. In the present test example, a time step $k = 0.5\Delta x$ and the duality method parameter $\omega = 2$ have been considered. For $\Lambda = 300$ and $\lambda = 0$ or 1, the computed quadratic error between the numerical and the analytical solutions for different uniform meshes, is shown in Fig. 1.

Notice that a quadratic error $\mathbf{O}(\Delta x)$ is gained, which agrees for the choice $k = 0.5\Delta x$ with the order $\mathbf{O}(\Delta x + \Delta x^2/k + k)$ stated in [4] for the stationary linear advection–diffusion equation.

Test 2. In order to validate the numerical algorithm by a more realistic test concerning the compressible Reynolds equation, we have considered the one proposed in Jai [11]. More precisely, the boundary value

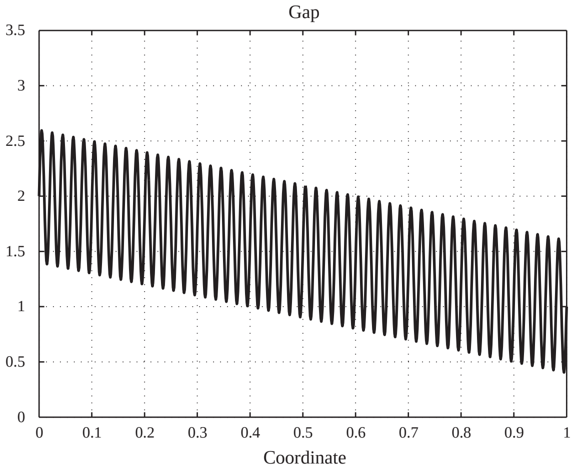

Fig. 2. Gap function in the rough case with $e = 0.6$ and $v = 0.02$.

problem is

$$\Lambda \frac{\mathrm{d}}{\mathrm{d}x}(h\,p) - \frac{\mathrm{d}}{\mathrm{d}x}\left(\lambda h^2 \frac{\mathrm{d}p}{\mathrm{d}x} + h^3 p \frac{\mathrm{d}p}{\mathrm{d}x}\right) = 0, \quad x \in (0, 1),$$
$$p(0) = p(1) = 1,$$

where the author has taken

$$h(x) = 2 - x + e \sin\left(2\pi \frac{x}{v}\right)$$

as the function that describes the gap (see Fig. 2). The oscillatory term is included in order to simulate the periodic roughness of a hard disk device; this artificial roughness is designed for a better control of the interfacial static force condition that exists between recording head and disk surface during the rotational start-up. Following the author, we have taken $e = 0.6$ and $v = 0.02$ for the roughness amplitude and the period, respectively. Moreover, the parameters $\Lambda = 300$ and $\lambda = 0$ are also considered.

For the numerical solution, the algorithm parameters $\Delta x = 10^{-3}$, $k = 0.5\Delta x$ and $\omega = 2$ have been chosen. The computed solution is shown in Fig. 3 and presents a qualitative and quantitative agreement with the one in [11]. To be noticed is the increasing of pressure for decreasing gap.

We also present in Fig. 4 the pressure distribution in the roughless case (corresponding to $e = 0$) for $\Lambda = 300$ and $\lambda = 0$. The numerical parameters are $\Delta x = 10^{-2}$, $k = 0.5\Delta x$ and $\omega = 2$.

5. Conclusions and future work

In this paper, the authors propose a new method for the numerical solution of the compressible Reynolds equation with first-order slip flow terms which models the air pressure in hard-disk devices. A characteristics method to deal with the convection dominated feature and the presence of sharp pressure gradients

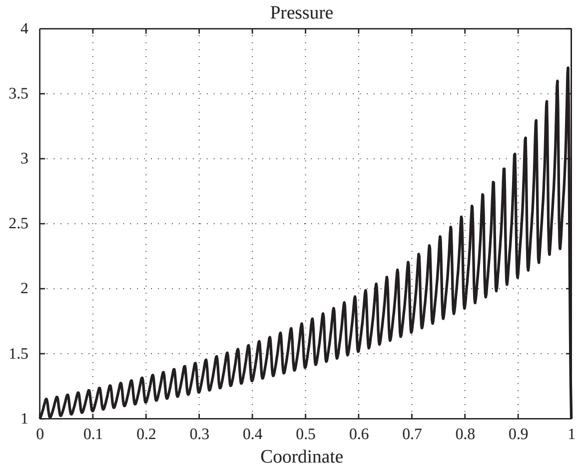

Fig. 3. Approximation of the pressure distribution in Test 2 in the rough case with $e = 0.6$ and $v = 0.02$.

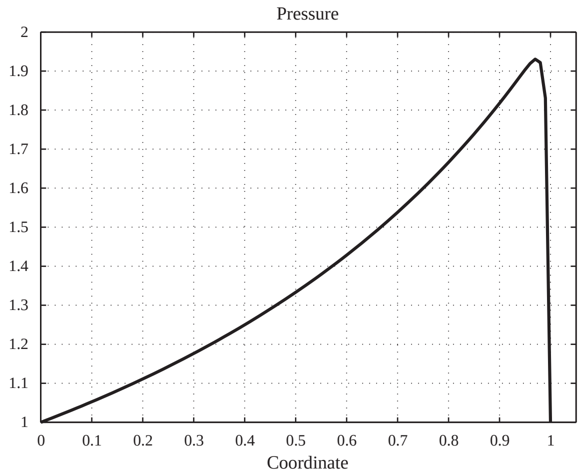

Fig. 4. Approximation of the pressure distribution in Test 2 in the roughless case.

has been applied. Moreover, an original duality method is proposed for the nonlinear diffusive term, which is written by means of a suitable maximal monotone operator.

The numerical algorithm is validated with two test examples: one with analytical solution and a second one issued from the literature.

On one hand, the numerical technique can be extended to a higher spatial dimension, as the model proposed in [9]. On the other hand, the proposed method for the hydrodynamic problem is now being coupled with a numerical method for solving the elastic rod model (1.2), (1.5), which governs the magnetic tape or another flexible storage media. The steady state solution for the model (1.1)–(1.5) could be obtained as the limit of a fixed point iteration between the elastic and the hydrodynamic problems.

Finally, the theoretical convergence analysis of the algorithm (3.16) to (p^{m+1}, θ^{m+1}) in this particular nonlinear diffusion problem is now being studied by the authors.

Acknowledgements

The authors would like to thank the Ministerio de Ciencia y Tecnología (Project BFM2001-3261-C02-02) and Xunta de Galicia (Project PGIDIT-02-PXIC-10503-PN) for the financial support to this work.

References

[1] G. Bayada, M. Chambat, C. Vázquez, Characteristics method for the formulation and computation of a free boundary cavitation problem, J. Comput. Appl. Math. 98 (1998) 191–212.
[2] M. Bercovier, O. Pironneau, V. Sastri, Finite elements and characteristics for some parabolic-hyperbolic problems, Appl. Math. Modelling 7 (1983) 89–96.
[3] A. Bermúdez, Un método numérico para la resolución de ecuaciones con varios términos no lineales. Aplicación a un problema de flujo de gas en un conducto, Rev. Real Acad. Cienc. Exact. Fis. Natur (Esp.) 78 (1981) 89–96.
[4] A. Bermúdez, J. Durany, La méthode des caractéristiques pour les problèmes de convection-diffusion stationnaires, Math. Model. Numer. Anal. 21 (1987) 7–26.
[5] A. Bermúdez, C. Moreno, Duality methods for solving variational inequalities, Comput. Math. Appl. 7 (1981) 43–58.
[6] B. Bhushan, Tribology and Mechanics of Magnetic Storage Devices, Springer, New York, 1990.
[7] H. Brézis, Analyse Fonctionnelle, Masson, Paris, 1983.
[8] M. Chipot, M. Luskin, Existence and uniqueness of solutions to the compressible Reynolds lubrication equation, SIAM J. Math. Anal. 17 (1986) 1390–1399.
[9] A. Friedman, Mathematics in Industrial Problems, Part 7, IMA Vol. 67, Springer, New York, 1994.
[10] A. Friedman, B. Hu, Head–media interaction in magnetic recording, Arch. Rational Mech. Anal. 140 (1997) 79–101.
[11] M. Jai, Homogenization and two-scale convergence of the compressible Reynolds lubrification equation modelling the flying characteristics of a rough magnetic head over a rough rigid-disk surface, Math. Model. Numer. Anal. 29 (1995) 199–233.
[12] M. Jai, Existence and uniqueness of solutions for parabolic nonlinear Reynolds equations, Nonlinear Anal. Theor. Methods Appl. 43 (2001) 655–682.
[13] C.A. Lacey, F.E. Talke, A tightly coupled numerical foil bearing solution, IEEE Trans. Magnetics 26 (1990) 3039–3043.
[14] E. Marusik-Paloka, Analysis of nonlinear evolutional Reynolds model for air lubrication of magnetic hard-disk via elliptic regularization, Nonlinear Anal.: Real World Appl. 4 (2003) 325–333.
[15] C. Parés, J. Macías, M. Castro, Duality methods with an automatic choice of parameters, Numer. Math. 89 (2001) 161–189.